FULL PAPER

Dalton
www.rsc.org/dalton

# Supramolecular systems built from phenylcyanamido ligands. Syntheses, crystal structures and magnetic properties

**Albert Escuer,*[a] Franz A. Mautner,[b] Núria Sanz[a] and Ramon Vicente[a]**

[a] *Departament de Química Inorgànica, Universitat de Barcelona, Martí Franqués 1-11, 08028 Barcelona, Spain. E-mail: albert.escuer@qi.ub.es*

[b] *Institut für Physikalische und Theoretische Chemie, Technische Universität Graz, A-8010 Graz, Austria. E-mail: Mautner@ptc.tu-graz.ac.at*

***Received 16th January 2003, Accepted 28th March 2003***
***First published as an Advance Article on the web 14th April 2003***

Several new $Mn^{II}$ compounds with X-phenylcyanamido (Xpcyd) and 2,2′-bipyrimidine (2,2′-bpm) bridging ligands of formula $[Mn(pcyd)(MeOH)(\mu\text{-}pcyd)(\mu\text{-}2,2'\text{-}bpm)_{0.5}]_n$ (**1**), $[Mn(3\text{-}Clpcyd)(MeOH)(\mu\text{-}3\text{-}Clpcyd)(\mu\text{-}2,2'\text{-}bpm)_{0.5}]_n$ (**2**), $(\mu\text{-}4\text{-}Clpcyd)_2[Mn(4\text{-}Clpcyd)(H_2O)(2,2'\text{-}bpm)]_2$ (**3**) and $[Mn(3\text{-}Fpcyd)(MeOH)(\mu\text{-}3\text{-}Fpcyd)(\mu\text{-}2,2'\text{-}bpm)_{0.5}]_n$ (**4**) have been synthesised and characterised. The one-dimensional compound $[Mn(pcyd)(MeOH)(\mu\text{-}pcyd)(\mu\text{-}2,2'\text{-}bpm)_{0.5}]_n$ (**1**) crystallises in the triclinic system, $P\bar{1}$ space group and the dinuclear compound $(\mu\text{-}4\text{-}Clpcyd)_2[Mn(4\text{-}Clpcyd)(H_2O)\text{-}(2,2'\text{-}bpm)]_2$ (**3**) crystallises in the orthorhombic system, $P2_12_12_1$ space group. The two compounds contain the unusual end-to-end cyanamide bridge and give supramolecular 2-D networks by means of H-bonds. Susceptibility measurements on compounds **1**–**4** reveal moderate antiferromagnetic coupling in all cases. Coupling constants related to the phenylcyanamido bridges are compared with the superexchange model recently proposed for ligands of this kind.

## Introduction

In the last few years, a large number of papers have been published about polynuclear or *n*-dimensional systems derived from pseudo-halides, mainly azido ligands[1] or dicyanamide.[2] These systems have provided a great variety of structural topologies and magnetic properties, including ferro-, antiferro- (homogeneous or alternating) or in some few cases, ferrimagnetic systems.[3]

In contrast, phenylcyanamide (pcyd) ligands are practically unexplored from the synthetic or magnetic point of view, in spite of the evident similarities of the –NCN group with the above-mentioned ligands. The majority of the work performed with Xpcyd derivatives has been done with $Ru^{III}$ and only a few mononuclear or dinuclear systems derived from the cations $Ag^{I}$, $Cu^{I}$ or $Cu^{II}$ have been reported.[4]

Recent articles have dealt with the theory and synthesis of bis-cyanamido systems, which may have interesting magnetic properties.[4,5]

Focusing our attention on the Xpcyd ligands containing only one cyanamido group we have reported a variety of structural topologies for the $Mn^{II}$–Xpcyd system, from dinuclear to 1-D or 2-D systems and the first magnetic measurements of compounds containing ligands of this kind.[6] We concluded, from experimental and MO calculations, that the $\mu_{1,3}$-NCN Xpcyd ligands have an intermediate place between azido and dicyanamido as superexchange mediators, giving moderate antiferromagnetic coupling. We also presented experimental evidence of the ability of these ligands to generate H-bond networks by means of the N-amide atom.[6]

Following our work with this family of ligands, we now report four new $Mn^{II}$–Xpcyd compounds in combination with the 2,2′-bipyrimidine ligand (2,2′-bpm). The new systems consist of dinuclear or alternating chains in which the H-bonds again play a central role in generating 2-D supramolecular arrangments. Measurement of their magnetic properties adds new data to check the recently proposed coupling model.[6]

## Experimental

### Physical measurements

Magnetic susceptibility measurements were carried out on polycrystalline samples with a DSM8 pendulum susceptometer working in the range 4–300 K, under magnetic fields of approximately 1 T or in a SQUID instrument in the range 2–300 K under an external field of 0.1 T. Diamagnetic corrections were estimated from Pascal Tables. The infrared spectra (4000–400 $cm^{-1}$) were recorded from KBr pellets on a Nicolet 520 FTIR spectrophotometer. EPR spectra were recorded with a Bruker ES200 spectrometer at X-band frequency. Thermogravimetric measurements were carried out in a Mettler TG 50 instrument at a heating rate of 10 °C $min^{-1}$.

### Synthesis

Neutral pcyd, 3-fluoro-, 3-chloro- and 4-chloro-phenylcyanamide (XpcydH) were prepared in all cases by desulfurization of the corresponding X-phenylthiourea with lead acetate, following the general synthetic procedure described for the halogeno-derivatives of phenylcyanamide.[7]

$[Mn(pcyd)(MeOH)(\mu\text{-}pcyd)(\mu\text{-}2,2'\text{-}bpm)_{0.5}]_n$ (**1**) was prepared by reaction of a solution of manganese nitrate hexahydrate (1 mmol) and 2,2′-bipyrimidine (0.5 mmol) in 50 mL of methanol with a solution of pcydH (2 mmol) in 6 mL of NaOH 0.2 M to deprotonate the ligand. After the reagents were mixed, the resulting clear solution was allowed to evaporate, giving a yellowish-orange crystalline compound suitable for X-ray measurements in three days. Yield 20%. Elemental analysis calcd. (%) for $MnC_{19}H_{17}N_6O$ (400.3): C 57.0, H 4.3, N 21.0; found C 57.4, H 4.3, N 21.0.

$[Mn(3\text{-}Clpcyd)(MeOH)(\mu\text{-}3\text{-}Clpcyd)(\mu\text{-}2,2'\text{-}bpm)_{0.5}]_n$ (**2**), $(\mu\text{-}4\text{-}Clpcyd)_2[Mn(4\text{-}Clpcyd)(H_2O)(2,2'\text{-}bpm)]_2$ (**3**) and $[Mn(3\text{-}Fpcyd)(MeOH)(\mu\text{-}3\text{-}Fpcyd)(\mu\text{-}2,2'\text{-}bpm)_{0.5}]_n$ (**4**): the method was the same as that indicated for compound **1**, using 2 mmol of the corresponding XpcydH ligand instead of the 2 mmol of pcydH. Yields of the corresponding yellow products were 41, 15 and 17% respectively. Elemental analysis calcd. (%) for **2** $MnC_{19}H_{15}Cl_2N_6O$ (469.2): C 48.6, H 3.2, N 17.9; found C 48.1, H 3.1, N 18.1; elemental analysis calcd. (%) for **3**, $Mn_2C_{44}\text{-}H_{32}Cl_4N_{16}O_2$ (1068.5): C 49.5, H 3.0, N 21.0; found: C 49.2, H 2.9, N 20.9; elemental analysis calcd. (%) for **4**, $MnC_{19}\text{-}H_{15}F_2N_6O$ (436.3): C 52.3, H 3.5, N 19.3; found: C 52.3, H 3.4, N 19.4. Crystals suitable for X-ray crystal diffraction were also obtained for **3**. In all cases, the small crystals degrade slowly once removed from the mother solution.

For compounds **1**–**4**, thermogravimetric analysis performed between 30 and 500 °C with a heating rate of 10 °C $min^{-1}$ shows

DOI: 10.1039/b300603d

**Table 1** Crystal data and structure refinement for [Mn(pcyd)(MeOH)(μ-pcyd)(μ-2,2′-bpm)$_{0.5}$]$_n$ (**1**) and (μ-4-Clpcyd)$_2$[Mn(4-Clpcyd)(H$_2$O)(2,2′-bpm)]$_2$ (**3**)

| | **1** | **3** |
|---|---|---|
| Formula | $C_{76}H_{68}Mn_4N_{24}O_4$ | $C_{44}H_{32}Cl_4Mn_2N_{16}O_2$ |
| $M$ | 1601.30 | 1068.54 |
| Crystal system | Triclinic | Orthorhombic |
| Space group | $P\bar{1}$ | $P2_12_12_1$ |
| $a$/Å | 10.931(4) | 8.365(4) |
| $b$/Å | 17.269(9) | 20.646(8) |
| $c$/Å | 19.955(9) | 26.163(9) |
| $\alpha$/° | 85.08(3) | 90 |
| $\beta$/° | 89.47(3) | 90 |
| $\gamma$/° | 86.35(3) | 90 |
| $V$/Å$^3$ | 3745(3) | 4519(3) |
| $Z$ | 2 | 4 |
| $T$/°C | −185(2) | −185(2) |
| $\rho_{calc}$/g cm$^{-3}$ | 1.420 | 1.571 |
| $\mu$(Mo-K$_\alpha$)/mm$^{-1}$ | 0.726 | 0.855 |
| $R^a$ | 0.0788 | 0.0569 |
| $\omega R^{2\,b}$ | 0.2241 $^b$ | 0.1468 |

$^a$ $R(F_o) = \Sigma F_o - F_c/\Sigma F_o$. $^b$ $\omega R\,(F_o)^2 = \{\Sigma[\omega((F_o)^2 - (F_c)^2)^2]/\Sigma[\omega((F_o)^4]\}^{1/2}$.

well-defined weight losses at moderate temperatures due to the coordinated solvents. Compounds **1**, **2** and **4** show similar thermal behavior: for the three compounds the first mass loss (8.4% for **1**, poorly defined and overlapping the decomposition loss for **2**, and 7.7% for **4**) were observed at 80–150 °C, 80–160 °C and 60–150 °C respectively, followed by decomposition of the compound above 240 °C (**1** and **2**) or 210 °C (**4**). Compound **3** shows the first mass loss from 150 °C due to the coordinated water molecules overlapping the decomposition of the compound above 200 °C. Compounds **1**, **2** and **4** may lose coordinated methanol at room temperature when finely powdered samples are stored for several days. To avoid errors in the magnetic measurements, the corresponding samples were freshly extracted from the mother solutions, dried and powdered just prior to performing the measurements.

### IR spectra

The most characteristic absorptions due to the Xpcyd ligands are those relating to the stretching of the CN group of the cyanamide fragment. For the free ligands these absorptions appear as strong bands in a short wavenumber range (2228, 2239, 2238 and 2235 cm$^{-1}$ for Hpcyd, 3-Clpcyd, 4-Clpcyd and 3-Fpcyd respectively), which shifts to *ca*. 2120 cm$^{-1}$ for the deprotonated Xpcyd$^-$ anions. The four reported compounds exhibits two strong signals at 2167–2127 cm$^{-1}$ for **1**, 2166–2127 cm$^{-1}$ for **2**, 2157–2118 cm$^{-1}$ for **3** and 2167–2130 cm$^{-1}$ for **4**, indicating two kinds of Xpcyd ligand in these compounds. According to the previous data, these values agree with $\mu_{1,3}$-Xpcyd ligands (signal close to 2160 cm$^{-1}$) and terminal, N-nitrile bonded Xpcyd ligands (signal at lower wavenumbers).

### X-Ray data collection for 1 and 3

The X-ray single-crystal data for [Mn(pcyd)(MeOH)(μ-pcyd)(μ-2,2′-bpm)$_{0.5}$]$_n$ (**1**) and (μ-4-Clpycd)$_2$[Mn(4-Clpcyd)(H$_2$O)(2,2′-bpm)]$_2$ (**3**) were collected on a modified STOE four-circle diffractometer. The crystallographic data, conditions retained for the intensity data collection, and some features of the structure refinement are listed in Table 1. Graphite-monochromatized Mo-Kα radiation ($\lambda$ = 0.71069 Å) with the $\omega$-scan technique was used to collect the data sets. Corrections were applied for Lorentz-polarization effects and intensity decay. The structures were solved by direct methods and subsequent Fourier analyses. Anisotropic displacement parameters were applied to non-hydrogen atoms, in full-matrix least-squares refinements based on $F^2$, except for the C atoms in the case of **1**, in order to keep the ratio of observed data/refined parameters > 10 : 1. The hydrogen atoms were assigned with isotropic displacement factors and included in the final refinement cycles by using geometrical restraints. For **3** a racemic twin refinement was also applied. The programs SHELXS-86,[8] SHELXL-93[9] incorporated in the SHELXTL/PC program package[10] and PLUTON-92[11] were used for computations. Selected bond parameters for **1** and **3** are given in Tables 2 and 3 respectively.

CCDC reference numbers 201209 for **1** and 201210 for **3**.

See http://www.rsc.org/suppdata/dt/b3/b300603d/ for crystallographic files in CIF or other electronic format.

**Table 2** Selected bond lengths [Å] and angles [°] for [Mn(pcyd)(MeOH)(μ-pcyd)(μ-2,2′-bpm)$_{0.5}$]$_n$ (**1**)

| | | | |
|---|---|---|---|
| Manganese environment | | | |
| Mn(1)–O(1) | 2.217(6) | Mn(2)–O(2) | 2.221(6) |
| Mn(1)–N(2) | 2.307(7) | Mn(2)–N(6) | 2.300(7) |
| Mn(1)–N(3) | 2.127(8) | Mn(2)–N(7) | 2.118(8) |
| Mn(1)–N(5) | 2.128(7) | Mn(2)–N(1) | 2.151(7) |
| Mn(1)–N(23) | 2.296(6) | Mn(2)–N(9) | 2.327(6) |
| Mn(1)–N(24_a) | 2.318(7) | Mn(2)–N(11) | 2.322(7) |
| Mn(3)–O(3) | 2.197(6) | Mn(4)–O(4) | 2.194(6) |
| Mn(3)–N(14) | 2.265(7) | Mn(4)–N(18) | 2.249(7) |
| Mn(3)–N(15) | 2.118(8) | Mn(4)–N(19) | 2.121(8) |
| Mn(3)–N(17) | 2.136(7) | Mn(4)–N(13) | 2.171(7) |
| Mn(3)–N(12) | 2.339(6) | Mn(4)–N(22_b) | 2.349(6) |
| Mn(3)–N(10) | 2.325(7) | Mn(4)–N(21) | 2.316(7) |
| pcyd ligands | | | |
| N(1)–C(1) | 1.185(11) | N(5)–C(15) | 1.150(11) |
| C(1)–N(2) | 1.273(11) | C(15)–N(6) | 1.306(11) |
| C(2)–N(2) | 1.420(10) | C(16)–N(6) | 1.432(10) |
| N(13)–C(37) | 1.158(11) | N(17)–C(51) | 1.166(11) |
| C(37)–N(14) | 1.284(11) | C(51)–N(18) | 1.294(11) |
| C(38)–N(14) | 1.437(10) | C(52)–N(18) | 1.427(10) |
| N(3)–C(8) | 1.162(11) | N(7)–C(22) | 1.182(11) |
| C(8)–N(4) | 1.285(11) | C(22)–N(8) | 1.284(10) |
| C(9)–N(4) | 1.425(11) | C(23)–N(8) | 1.429(11) |
| N(15)–C(44) | 1.171(11) | N(19)–C(58) | 1.167(11) |
| C(44)–N(16) | 1.271(10) | C(58)–N(20) | 1.289(11) |
| C(45)–N(16) | 1.424(11) | C(59)–N(20) | 1.416(11) |
| Mn–pcyd bond angles | | | |
| Mn(1)–N(2)–C(1) | 112.5(6) | Mn(2)–N(6)–C(15) | 110.5(5) |
| C(1)–N(1)–Mn(2) | 160.0(7) | C(15)–N(5)–Mn(1) | 161.2(7) |
| Mn(3)–N(14)–C(37) | 115.9(6) | Mn(4)–N(18)–C(51) | 113.5(6) |
| C(37)–N(13)–Mn(4) | 153.9(7) | C(51)–N(17)–Mn(3) | 154.0(7) |
| Mn(1)–N(3)–C(8) | 152.4(6) | Mn(2)–N(7)–C(22) | 144,5(6) |
| Mn(3)–N(15)–C(44) | 149.8(6) | Mn(4)–N(19)–C(58) | 141,3(7) |

**Table 3** Selected bond lengths [Å] and angles [°] for (μ-4-Clpcyd)$_2$[Mn(4-Clpcyd)(H$_2$O) (2,2′-bpm)]$_2$ (**3**)

| | | | |
|---|---|---|---|
| Manganese environment | | | |
| Mn(1)–O(1) | 2.163(5) | Mn(2)–O(2) | 2.153(5) |
| Mn(1)–N(4) | 2.295(6) | Mn(2)–N(2) | 2.297(6) |
| Mn(1)–N(1) | 2.148(5) | Mn(2)–N(3) | 2.145(5) |
| Mn(1)–N(5) | 2.134(6) | Mn(2)–N(7) | 2.130(6) |
| Mn(1)–N(9) | 2.346(6) | Mn(2)–N(11) | 2.345(6) |
| Mn(1)–N(10) | 2.275(4) | Mn(2)–N(12) | 2.259(4) |
| 4-Clpcyd ligands | | | |
| N(1)–C(1) | 1.166(8) | N(3)–C(8) | 1.168(8) |
| C(1)–N(2) | 1.275(8) | C(8)–N(4) | 1.277(8) |
| N(2)–C(2) | 1.419(7) | N(4)–C(9) | 1.406(7) |
| N(5)–C(15) | 1.153(8) | N(7)–C(22) | 1.172(9) |
| C(15)–N(6) | 1.268(8) | C(22)–N(8) | 1.267(8) |
| N(6)–C(16) | 1.390(7) | N(8)–C(23) | 1.389(7) |
| Mn–4-Clpcyd bond angles | | | |
| Mn(1)–N(1)–C(1) | 143.7(5) | Mn(2)–N(3)–C(8) | 140.0(5) |
| C(1)–N(2)–Mn(2) | 106.6(4) | C(8)–N(4)–Mn(1) | 105.8(4) |
| Mn(1)–N(5)–C(15) | 134.2(5) | Mn(2)–N(7)–C(22) | 132.3(5) |

## Results and discussion

### Crystal structure of $[Mn(pcyd)(MeOH)(\mu\text{-}pcyd)(\mu\text{-}2,2'\text{-}bpm)_{0.5}]_n$ (1)

The structure consists of a one-dimensional $Mn^{II}$ system bridged by double end-to-end phenylcyanamido and 2,2′-bipyrimidine in an alternating arrangement along the chain, Fig. 1. There are four crystallographically different $Mn^{II}$ atoms in the unit cell but the environment is very similar for all of them. Each manganese atom is coordinated by one bidentate 2,2′-bpm ligand, two N-atoms (one N-nitrile and one N-amido) from the two bridging phenylcyanamido ligands, one N-nitrile atom from one terminal phenylcianamido ligand and one O-atom of one solvent molecule (methanol). The octahedral coordination polyhedron shows several distortions related to each kind of ligand: bond distances (see Table 2) between the manganese atoms and the N-nitrile donors are between 2.118 and 2.151 Å, Mn–O distances lie in the range 2.194–2.221 Å, Mn–N-amide bonds are clearly longer than the Mn–N-nitrile (between 2.249 and 2.307 Å) and finally the Mn–N-bpm distances are between 2.296 and 2.349 Å. The major distortions in the bond angles correspond to the N–Mn–N bond angle related to the 2,2′-bpm ligand, which is between 70.7 and 71.8°, and to the *trans* angle determined for the N-nitile–Mn–N-bpm atoms, which has the minimum value of 158.3(2)° for N(3)–Mn(1)–N(23). As is commonly found for phenyl–cyanamido ligands,[4,6] Mn–N–nitrile bond distances are shorter than the Mn–N-amide and C–N-nitrile–Mn bond angles are also larger than the C–N-amide–Mn angles. Mn–N–C bond angles for the bridging pcyd ligands lie between 153.4 and 161.2° for the N-nitrile, whereas that corresponding to the amide fragment lies between 110.5 and 115.9°. The phenyl rings of the bridging cyanamido ligands are not coplanar with the NCN fragment, being rotated between 13.6 and 29.6°.

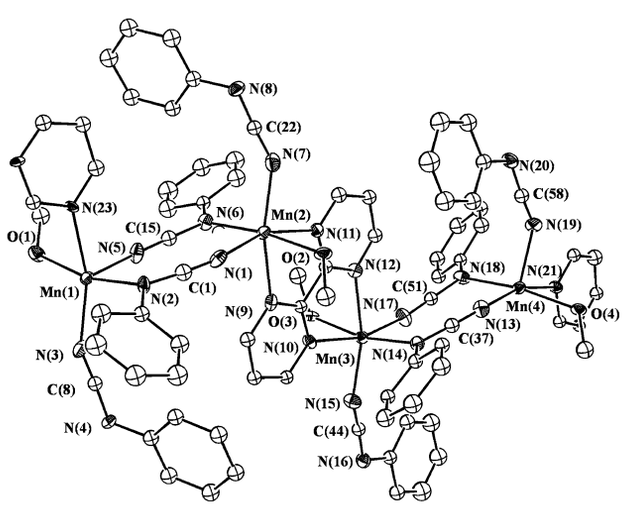


**Fig. 1** ORTEP[15] labelled plot (probability 40%) for $[Mn(pcyd)(MeOH)(\mu\text{-}pcyd)(\mu\text{-}2,2'\text{-}bpm)_{0.5}]_n$ (**1**). For the sake of clarity, only the labels for the coordination sphere of the $Mn^{II}$ cations and the NCN groups are shown.

The $Mn–(NCN)_2–Mn$ eight-membered rings show a different chair distortion evidenced by the dihedral angles between the main plane $(NCN)_2$ and the corresponding N–Mn–N planes: one of the rings is quasi-planar (dihedral angles between the mean plane and N(2)–Mn(1)–N(5) and N(1)–Mn(2)–N(6) are 3.3(3)° and 5.0(3)°), whereas the other ring is strongly distorted (dihedral angles between the mean $(NCN)_2$ plane and N(14)–Mn(3)–N(17) and N(13)–Mn(4)–N(18) are 16.0(3)° and 19.7(3)° respectively). Intrachain Mn ··· Mn distances are 5.445 and 5.413 Å through the cyanamido bridges and 6.164 and 6.185 Å through the 2,2′-bpm bridges.

### Crystal structure of $(\mu\text{-}4\text{-}Clpcyd)_2[Mn(4\text{-}Clpcyd)(H_2O)(2,2'\text{-}bpm)]_2$ (3).

In this case the structure consists of dinuclear $Mn^{II}$ units bridged by double 4-Clpcyd ligands coordinated in an end-to-end mode, Fig. 2. The coordination polyhedron of the manganese atoms is formed by two N-atoms from one bidentate 2,2′-bpm ligand, two N-atoms (one N-nitrile and one N-amido) from two bridging 4-Clpcyd ligands, one N-nitrile atom from one terminal 4-Clpcyd and one O-atom from one solvent molecule (water in this case). Similarly to compound **1**, there are several ligand-related distortions of the octahedral environment (see Table 3): Mn–N-nitrile and $Mn–OH_2$ bond distances (around 2.139 and 2.158 Å) are shorter than Mn–N-amide and Mn–N-2,2′-bpm (comprised in the 2.259–2.346 Å range). N–Mn–N bond angles determined by the 2,2′-bpm ligand are also around 71°. Coordination of the bridging 4-Clpcyd is strongly asymmetric, the Mn(1)–N(1)–C(1) and Mn(2)–N(3)–C(8) bond angles involving N-nitrile atoms (143.7(5)° and 140.0(5)°) being larger than Mn(1)–N(4)–C(8) and Mn(2)–(N2)–C(1) bond angles involving N-amide atoms (105.8(4)° and 106.6(4)°). 4-Clpcyd ligands are quite planar, but phenyl rings are rotated along the NCN axis forming a dihedral angle between the aromatic rings and the main $(NCN)_2$ plane close to 36°. The $Mn–(NCN)_2–Mn$ ring shows a strong chair distortion, evidenced by the dihedral angle between the N(1)–Mn(1)–N(4) and N(2)–Mn(2)–N(3) planes and the main $(NCN)_2$ plane (36.2(2)° and 37.9(2)° respectively). The intramolecular Mn ··· Mn distance is 5.139(2) Å.

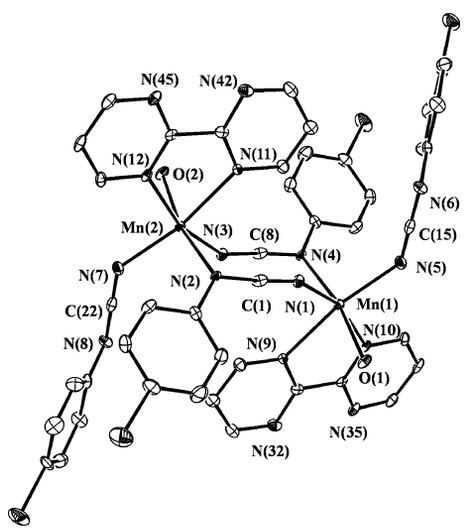


**Fig. 2** ORTEP labelled plot (probability 40%) for $(\mu\text{-}4\text{-}Clpcyd)_2[Mn(4\text{-}Clpcyd)(H_2O)(2,2'\text{-}bpm)]_2$ (**3**). For the sake of clarity, only the labels for the coordination sphere of the $Mn^{II}$ cations and the NCN groups are shown.

### Supramolecular H-bonded networks

As we pointed out for the first Mn–Xpcyd systems,[6] when the complex contains terminal pcyd ligands coordinated by the N-nitrile atom, the second N-amide atom shows a strong tendency to generate H-bonds with –OH groups from solvent molecules. In this previous paper we showed that dinuclear entities allow 1-D H-bonded systems or even mononuclear compounds such as $[Mn(H_2O)_2(4\text{-}bzpy)_2(3\text{-}Clpcyd)_2]$ (4-bzpy = 4-benzoylpyridine) containing two solvent molecules coordinated to the manganese atom generates 2-D H-bonded networks. In this case, compound **1** follows the same trends giving a 2-D superstructure, Fig. 3, by means of hydrogen bonds between the N-amide atoms N(4), N(8), N(16), N(20) of one of the chains and O(4), O(2), O(3), O(1) from the MeOH coordinated molecules of neighbouring chains, respectively. In all cases N ··· O distances lie between 2.671 and 2.708 Å with

**Table 4** Distances [Å] and bond angles [°] for the H-bonds present in compounds **1** and **3**

| | O–H | H ··· N | O ··· N | O–H ··· N |
|---|---|---|---|---|
| Compound **1** | | | | |
| O(1)–H(1O) ··· N(20) | 0.87 | 1.80 | 2.671(9) | 175 |
| O(2)–H(2O) ··· N(8) | 0.88 | 1.85 | 2.708(9) | 164 |
| O(3)–H(3O) ··· N(16) | 0.88 | 1.84 | 2.676(9) | 160 |
| O(4)–H(4O) ··· N(4) | 0.88 | 1.84 | 2.704(9) | 166 |
| Compound **2** | | | | |
| O(1)–H(1) ··· N(42) | 0.85 | 2.49 | 3.031(6) | 122 |
| O(1)–H(1) ··· N(45) | 0.85 | 2.20 | 3.020(7) | 163 |
| O(1)–H(2) ··· N(8) | 0.85 | 1.92 | 2.750(7) | 164 |
| O(2)–H(8) ··· N(6) | 0.84 | 1.91 | 2.746(7) | 169 |
| O(2)–H(9) ··· N(32) | 0.84 | 2.54 | 3.096(6) | 125 |
| O(2)–H(9) ··· N(35) | 0.84 | 2.10 | 2.922(7) | 165 |

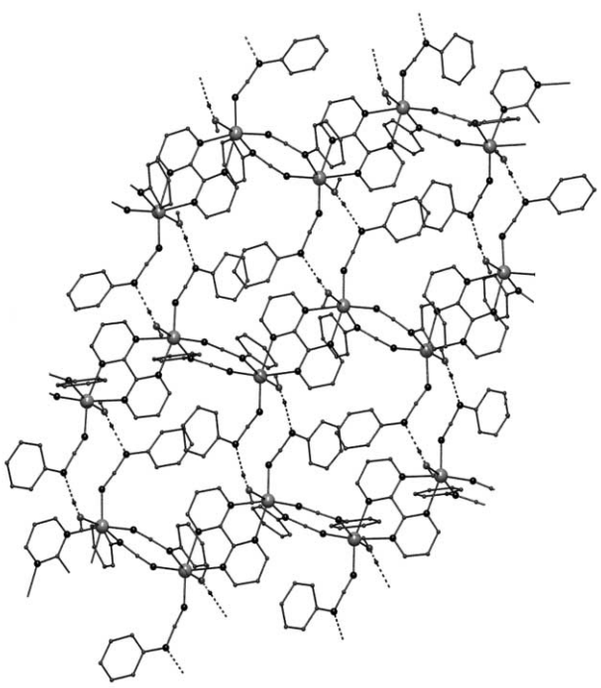

**Fig. 3** Two-dimensional H-bond network for compound **1**. The alternating 2,2′-bpm/pcyd chains link between them by means of the H-bonds (dashed lines) between the N-amide atoms of terminal pcyd ligands and the O-atom from the coordinated methanol.

O–H ··· N angles around 166°, Table 4. Mn ··· Mn distances through the H-bonded directions are in the range 6.847–7.094 Å. The minimum interplane Mn ··· Mn distance is 9.903 Å.

In compound **3**, N-amide atoms are also involved in a network of H-bonds, but in this case, the two non-coordinated N-atoms from the 2,2′-bpm ligand also participate in the supramolecular interactions, giving a more complicated pattern of interactions that allow the final 2-D planes. The 2-D network is obtained from discrete dinuclear molecules by means of the four H-atoms of the coordinated water molecules. H(2) and H(8) link to the N-amide atoms N(8) and N(6) whereas H(1) and H(9) link two N-atoms from 2,2′-bpm ligands. The two-dimensional arrangement may be envisaged as 1-D alternating pseudo-chains (pcyd bridges and double H-bond involving the N-amide atoms) that are joined by the H-bonds involving the N-atoms of the 2,2′-bpm, Fig. 4.

### Susceptibility measurements and powder EPR spectrum

Magnetic measurements were performed on freshly powdered crystalline samples (see Experimental section). For all the compounds reported, moderately weak antiferromagnetic (AF) responses were observed, showing $\chi_M T$ values at room temperature slightly lower than the expected value for isolated $Mn^{II}$ ions. On cooling, $\chi_M T$ gradually decreased tending to zero at low temperature. Plots of $\chi_M$ *vs.* $T$ show a well defined maximum at 22 K, 15 K, 7.5 K and 18 K for compounds **1**–**4** respectively.

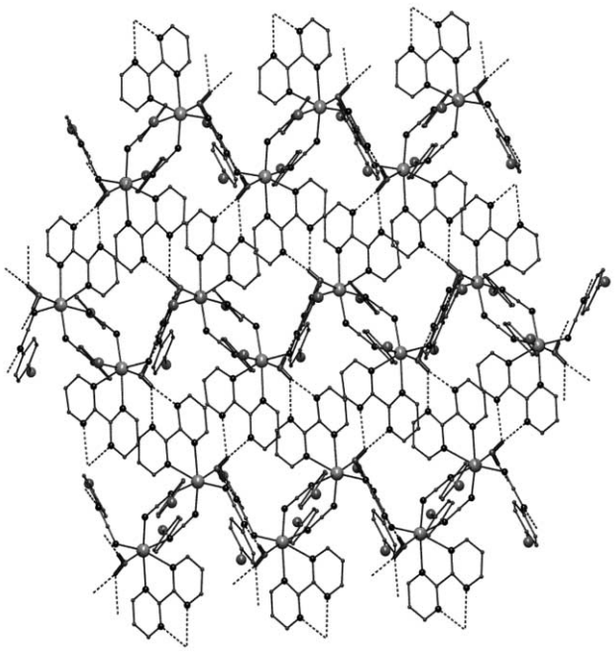

**Fig. 4** Two-dimensional H-bond network for compound **3**. In addition to the interaction with the N-amide atoms, the two non-coordinated N-atoms from the 2,2′-bpm ligands are also involved in the H-bond system.

EPR spectra for compounds **1**, **2** and **4** show a sharp isotropic band with a peak-to-peak increment ($\Delta_{pp}$) of 97, 135 and 84 G at room temperature, centered at $g$ = 2.01. On cooling below 100 K, $\Delta_{pp}$ increases, reaching values around 400 G. In contrast, compound **3** shows a signal centered at $g$ = 2.03 at room temperature with $\Delta_{pp}$ of 275 G, which gradually increases to 410 G at 4K. These data agree with the sharper signals found for 1-D systems compared with their dinuclear analogues, as reported elsewhere.[6,12]

The experimental susceptibility data of compound **1** (Fig. 5), were analyzed with the expression for an isotropic $S = 5/2$ alternating chain system derived by Drillon[13] from the Hamiltonian $H = -J_1\Sigma(S_{2i} \times S_{2i+1}) - J_2\Sigma(S_{2i} \times S_{2i+2})$ including a Weiss term to take into account the possible effect of the H-bonds. The best fit parameters were $J_1 = -4.3(1)$ cm$^{-1}$, $J_2 = -1.2(1)$ cm$^{-1}$, $g = 2.01(1)$ and a weak 0.4 K value for the Weiss constant. The $J_2$ coupling constant can be assigned to the 2,2′-bpm bridge, for which values around or slightly greater than 1 cm$^{-1}$ are typical for the Mn–(μ-2,2′-bpm)–Mn subunit.[14]

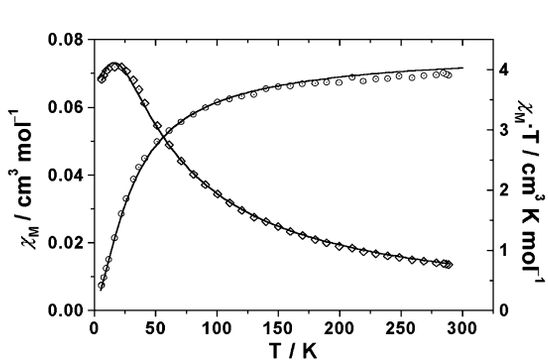


**Fig. 5** Susceptibility data for compound **1**. Solid lines correspond to the best fit indicated in the text.

Dinuclear compound **3** was fitted using the analytical expression derived from the isotropic Hamiltonian $H = -JS_1 \times S_2$, from which best fit values were $J = -1.9(1)$ cm$^{-1}$, $g = 2.03(1)$, Fig. 6.

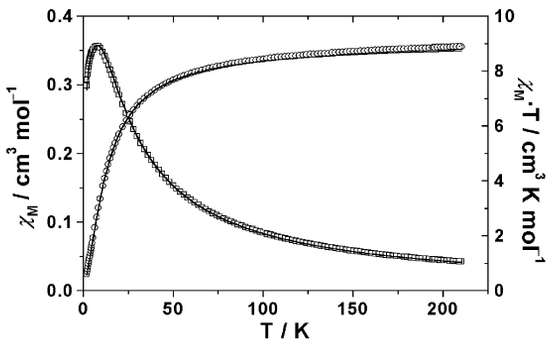


**Fig. 6** Susceptibility data for compound **3**. Solid lines correspond to the best fit indicated in the text.

For compounds **2** and **4** structural data are not available. Having found that the fit as dinuclear systems was poor and taking into account the similarities in the IR, thermal and EPR behavior and the shape of the susceptibility plots, we then fit the two compounds as alternating chains like compound **1**. Best fit parameters were $J_1 = -4.5(1)$ cm$^{-1}$, $J_2 = -1.2(1)$ cm$^{-1}$, $g = 2.00(1)$ for **2** and $J_1 = -4.3(1)$ cm$^{-1}$, $J_2 = -1.2(1)$ cm$^{-1}$, $g = 2.01(1)$ for compound **4**.

*J* values for compounds **1** and **3**, for which structural data are available, allowed us to check the validity of the general rules about the magnitude of the superexchange interaction recently reported for this kind of X-pcyd ligand.[6] Previous calculations show that the main factors favouring greater AF coupling are mainly related with the distortions in the Mn–$(NCN)_2$–Mn region: greater AF coupling are expected for systems in which the bridging region is not chair-distorted or in which the NCN–pcyd mean plane lies coplanar to the $(NCN)_2$ plane. As a minor effect, for similar distortions, the ligands with the X-atom in a *para* position (4-Xpcyd) should be more AF than pcyd or 3-Xpcyd ligands. Compound **1** shows higher values than **3** or the four previously reported systems with double R-pcyd bridges, in good accordance with the degree of chair distortion in the common bridging region Mn–$(NCN)_2$–Mn. Compound **1** has two non-equivalent units, one of them practically planar and the other showing a moderate chair distortion. In contrast, compound **3**, although the 4-Clpcyd favors greater AF coupling, shows the lowest *J* value due to the extreme chair distortion and the large deviation of the NCN–pcyd plane.

## Acknowledgements

A. E., R. V. and N. S. thank the Ministerio de Ciencia y Tecnología (Spain), project BQU2000/0791 for financial support. F. A. M. thanks Professors Belaj and Kratky (University of Graz) for use of experimental equipment and OENB (project 7967) for financial support.

## References

1 J. Ribas, A. Escuer, M. Monfort, R. Vicente, R. Cortés, L. Lezama and T. Rojo, *Coord. Chem. Rev.*, 1999, **193–195**, 1027.
2 P. M. Van der Werff, S. R. Batten, P. Jensen, B. Moubaraki and K. S. Murray, *Inorg. Chem.*, 2001, **40**, 1718; J. W. Raebiger, J. L. Manson, R. D. Sommer, U. Geiser, A. L. Rheingold and J. S. Miller, *Inorg. Chem.*, 2001, **40**, 2578; B. Vangdal, J. Carranza, F. Lloret, M. Julve and J. Sletten, *J. Chem. Soc., Dalton Trans.*, 2002, 566 and references therein.
3 M. A. M. Abu-Youssef, A. Escuer, M. A. S. Goher, F. A. Mautner, G. J. Reiβ and R. Vicente, *Angew. Chem., Int. Ed.*, 2000, **39**, 1624.
4 R. J. Crutchley, *Coord. Chem. Rev.*, 2001, **219–221**, 125.
5 A. M. Galibert, O. Cortadellas, B. Soula, B. Donnadieu and P. L. Fabre, *J. Chem. Soc., Dalton Trans.*, 2002, 3743.
6 A. Escuer, N. Sanz, R. Vicente and F. A. Mautner, *Inorg. Chem.*, 2003, **42**, 541.
7 B. R. Hollebone and R. S. Nyholm, *J. Chem. Soc. A*, 1971, 332.
8 G. M. Sheldrick, SHELXS-86, Program for the Solution of Crystal Structure, University of Göttingen, Germany, 1986.
9 G. M. Sheldrick, SHELXL-93, Program for the Refinement of Crystal Structure, University of Göttingen, Germany, 1993.
10 SHELXTL 5.03 (PC-Version), Program library for the Solution and Molecular Graphics, Siemens Analytical Instruments Division, Madison, WI, 1995.
11 A. L. Spek, PLUTON-92, University of Utrecht, The Netherlands, 1992.
12 M. A. M. Abu-Youssef, A. Escuer, D. Gatteschi, M. A. S. Goher, F. A. Mautner and R. Vicente, *Inorg. Chem.*, 1999, **38**, 5716.
13 R. Cortés, M. Drillon, X. Solans, L. Lezama and T. Rojo, *Inorg. Chem.*, 1997, **36**, 677.
14 G. de Munno, R. Ruiz, F. Lloret, J. Faus, R. Sessoli and M. Julve, *Inorg. Chem.*, 1995, **34**, 408; De Munno, M. Julve, G. Viau, F. Lloret, J. Faus and D. Viterbo, *Angew. Chem., Int. Ed. Engl.*, 1996, **35**, 1807; G. de Munno, T. Poerio, M. Julve, F. Lloret, G. Viau and A. Caneschi, *J. Chem. Soc., Dalton Trans.*, 1997, 601 and references therein.
15 M. N. Burnett and C. K. Johnson, ORTEP-III: Oak Ridge Thermal Ellipsoid Plot Program for Crystal Structure Illustrations, Report ORNL-6895, Oak Ridge National Laboratory, Oak Ridge, TN, 1996.